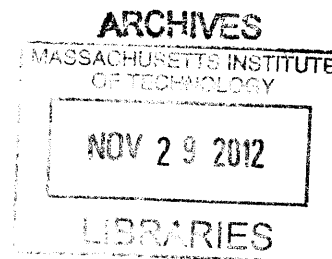# Theoretical Investigation of Stokes Shifts and Reaction Pathways

by

Laken M. Top

Associate of Arts, Science Option
Yakima Valley Community College, 2007

Bachelor of Science, Chemistry and Mathematics
University of Idaho, 2009

SUBMITTED TO THE DEPARTMENT OF CHEMISTRY   IN PARTIAL FULFILLMENT OF THE
REQUIREMENTS FOR THE DEGREE OF

MASTER OF SCIENCE IN CHEMISTRY
AT THE
MASSACHUSETTS INSTITUTE OF TECHNOLOGY

SEPTEMBER 2012

Signature of Author: _____
Department of Chemistry
July 12, 2012

Certified by: _____
Troy Van Voorhis
Associate Professor of Chemistry
Thesis Supervisor

Certified by: _____
Jeffrey C. Grossman
Associate Professor of Materials Science and Engineering
Thesis Supervisor

Accepted by: _____
Robert W. Field
Professor of Chemistry
Chairman, Department Committee on Graduate Theses

Theoretical Investigation of Stokes Shifts and Reaction Pathways

by

Laken M. Top

Submitted to the Department of Chemistry
on July 12, 2012, in partial fulfillment of the
requirements for the degree of
Master of Science in Chemistry

Abstract

Solar thermal fuels and fluorescent solar concentrators provide two ways in which the energy from the sun can be harnessed and stored. While much progress has been made in recent years, there is still much more to learn about the way that these applications work and more efficient materials are needed to make this a feasible source of renewable energy. Theoretical chemistry is a powerful tool which can provide insight into the processes involved and the properties of materials, allowing us to predict substances that might improve the efficiency of these devices. In this work, we explore how the delta self-consistent field method performs for the calculation of Stokes shifts for conjugated dyes. We also develop a new reaction path finding method which uses a combination of trigonometric functions and information about the initial and final states in the reaction to generate an approximate path. We show that this path finding method works well for several model systems including a seven atom Lennard-Jones cluster. The ability to calculate excited state properties at a reasonably low cost and to find convergent reaction pathways is extremely beneficial for understanding and improving solar devices.

Thesis Supervisor: Troy Van Voorhis
Title: Associate Professor of Chemistry

Thesis Supervisor: Jeffrey C. Grossman
Title: Associate Professor of Materials Science and Engineering

Acknowledgements

To Professor Troy Van Voorhis and Professor Jeffrey Grossman, my research advisors: thank you for being such wonderful mentors. Over the past three years, you have pushed me to grow in scientific understanding and critical thinking, while at the same time encouraging me to explore areas that I am passionate about. It has truly been a tremendous honor and privilege to be part of your research groups.

To Professor Jianshu Cao and the late Professor Robert Silbey, my committee members: thank you for sharing your wisdom and insight with me. Your availability and willingness to give assistance are very much appreciated.

To all of my coworkers in "the Zoo": thank you for making the office such a pleasant environment in which to work. Thank you for your tutoring, your constructive criticism, and your friendship.

To all of the lovely ladies in the Chemistry Education office: thank you for being the smiling faces that greeted lost, confused, and tired graduate students and helped them find their way. You made each and every one of us feel special when we needed it most.

To my parents, John and Wendy Top: thank you for instilling in me a love of learning. Thank you for never giving up on me, always pushing me to achieve my full potential, and encouraging me to pursue my goals. Without your love, I would not be where I am today.

To my siblings, Madison, Zachary, and Joram: thank you for being the comic relief in my life. Thank you for always welcoming me home with open arms. It is such a joy to be your big sister.

To my grandparents, David and LeRoyce Williams: thank you for your never-ending support and love. You are the greatest cheerleaders and the best grandparents anyone could ask for.

To Brad, my best friend and the love of my life: You've empathized with me through the trials and celebrated with me during the triumphs of grad school. Thank you for being such a pillar of support and encouragement in my life and for making me a better person. I look forward to a lifetime of love, adventure, and happiness together.

Contents

List of Figures

List of Tables

Chapter 1

Introduction

1.1   Renewable Energy Sources

Solar energy has become a very active area of research in recent years. The sun is a promising source of alternative energy, and much time has been spent developing ways to harness its power.

1.2   Solar Thermal Fuels

Research suggests that solar thermal fuels are a viable method and have the potential to supply enough heat for houses and engines. Solar fuels work by using chemical bonds to store energy. The molecules used for this purpose are photoactive and have two conformational states. When a molecule is in its lower energy geometry, it will absorb light which causes it to conformationally change to a higher energy state. This state is metastable and if supplied with a small amount of energy to overcome the activation barrier, the molecule will return to its lower energy conformation and release the energy stored in its bonds in the form of usable heat. This is an example of a photoswitching reaction. By exposing the molecule to light again, the process can reoccur, thus making the fuel reusable. Besides being renewable, solar fuels are advantageous because of their transportablity, their storage stability, and the lack of waste produced. The main challenge of implementing these fuels today is that most fuels decompose so quickly that they can only be reused for a short period of time, thus making this an expensive way to store energy.

1.3 Functionalized Carbon Nanotubes

It was recently proposed that carbon nanotubes could be used as a substrate to covalently bind photoswitch molecules to. This would increase their capacity to store energy as well as their thermal stability, thus causing them to degrade more slowly. The photomolecules adsorb to the carbon nanotubes in a close-packed, highly ordered fashion. This allows for an increase in photoisomer concentration as well as manipulation of molecular interactions. Azobenzene derivatives are commonly studied as photoswitch molecules and it has been shown that the effect of attaching them to carbon nanotubes could be extremely useful in solar fuel research (see Figure 1) [1].
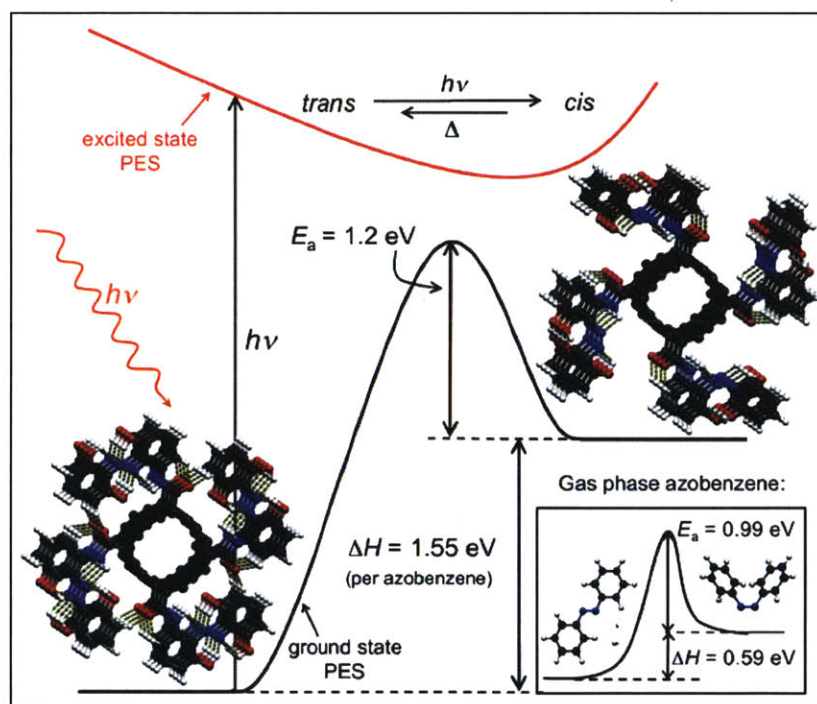
Figure 1. Illustration of the mechanics of solar thermal energy storage. The conformational change of an azobenzene photoswitch derivative is shown in the inset [1].

1.4 Fluorescent Solar Concentrators

Another popular area of solar research is in the field of light channeling devices, such as fluorescent (or luminescent) solar concentrators. These devices are made with transparent polymer sheets that are doped with luminescent agent molecules. The transparent sheets allow for the absorption of sunlight which is then fluoresced due to the luminescent agents. A

fraction of the emitted light is trapped between the sheets. This causes the light to move to the edges of the device where solar cells are located to use the concentrated radiation. These fluorescent solar concentrators could improve solar panels since they allow for the collection of sunlight over a larger area, while decreasing the number of expensive photovoltaic cells needed [2].

Stokes Shifts play an important role in the development of materials for these fluorescent solar concentrators. A Stokes shift is the difference between the absorption and emission peaks of a molecule (see Figure 2).

(a)   (b)
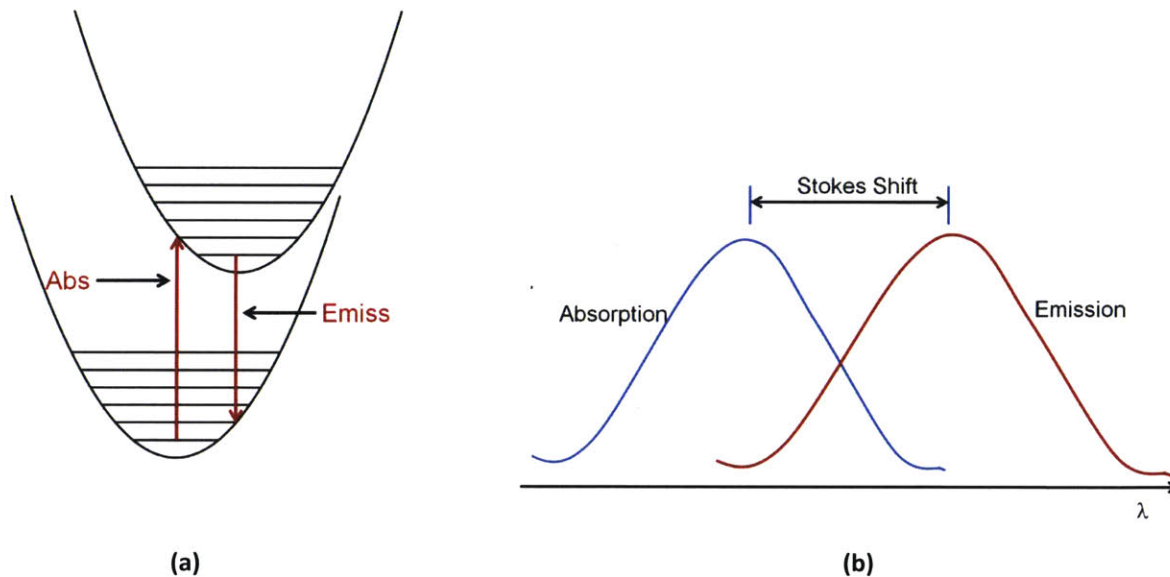
Figure 2. Two illustrations of Stokes shifts. In (a) the vertical transitions from ground state to excited state for both absorption and emission are shown, and in (b) the diagram illustrates the spectral shift of the emission peak from the absorption peak.

Since solar concentrators are sensitive to the reabsorption of photons, minimal overlap between the absorption and emission peaks is beneficial. In other words, materials with large Stokes shifts are optimal materials for these devices [3].

1.5   Challenges and Motivation

Theoretical chemistry can be a valuable tool for exploring new materials for solar fuels and fluorescent solar concentrators. Computational methods can act as predictive tools and suggest new directions for material development. The design of both solar fuels and concentrators depends heavily on the optical and electronic properties of the materials used. Computational tools for calculating electronic excited state properties have become very useful for this reason. In addition, information about reaction paths and transition states can be computed and provide insight into the mechanics of solar fuels. However, some challenges are encountered while computing electronic excited states of large molecules and finding transition states in chemical reactions is still a major struggle in the theoretical world. We would like to address these issues by developing a method to explore excited state reaction pathways that we could apply to solar applications.

Chapter 2

Investigation of Stokes Shifts Using the Delta Self-Consistent Field Method

2.1   Introduction

Over time several methods have been developed to study electronic excited state structure. Some of the oldest methods are semi empirical molecular orbital methods that are not quantitative, but are sufficient to predict trends. Later, *ab initio* methods became more widespread, but these remain too expensive for the large conjugated molecules typically used in solar applications. The primary method used for excited state electronic structure calculations today is time-dependent density functional theory (TDDFT), specifically within the adiabatic approximation, which provides a reasonable accuracy to expense ratio for many systems [4]. TDDFT can still be expensive for large systems however.

2.2   Delta Self-Consistent Field Method

In an attempt to alleviate this problem, as well as other issues with TDDFT, time-independent DFT alternatives have been proposed. One time-independent method is delta self-consistent field density functional theory (ΔSCF-DFT or ΔSCF) which is characterized by applying ground state DFT to non-Aufbau electronic configurations. Figure 3 illustrates the orbital relaxation of ΔSCF.

From the ground state, an electron is promoted to a higher orbital to enforce non-Aufbau occupation. The orbitals are then relaxed within the non-Aufbau constraint. The resulting ΔSCF orbitals are no longer spin eigenfunctions, and thus we need to take a linear combination of

calculated spin-mixed and spin-pure energies to acquire the energy for a singlet excited state [5].
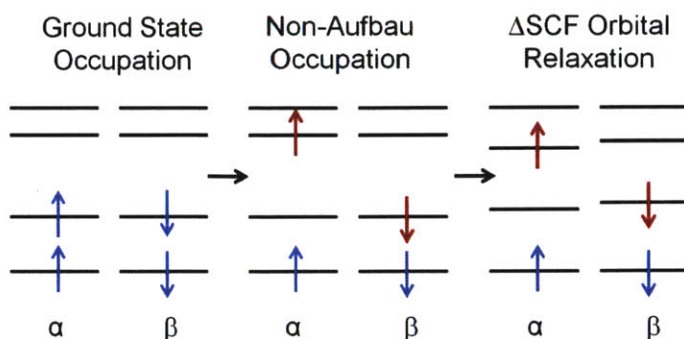
Figure 3. The orbitals used for calculating excited states within ΔSCF and the result of orbital relaxation.

Recently there has been evidence to suggest that ΔSCF is effective for Rydberg states, core excitations, solvent effects, and double excitations, which make it a great candidate for excited state calculations. ΔSCF also gives stationary densities (with respect to the molecular orbital coefficients) which are exact within the adiabatic approximation, which means it is local in time and uses the same exchange correlation functional for both the ground and excited states. ΔSCF has recently been shown to calculate the absorption of conjugated organic molecules with roughly the same accuracy as TDDFT. [6]

2.3   Calculation of Stokes Shifts for Conjugated Dyes

To continue the exploration of ΔSCF effectiveness, we have calculated Stokes shifts for a test set of 13 organic dye molecules using ΔSCF and TDDFT and compared the theoretical shifts to experimental values (see Table 1). We treated all molecules as if they were in the gas phase for simplicity, although some of the experimental numbers were measured in solvents. All of the solvents used in experiments, however, were nonpolar, and thus we can ignore them as nonpolar solvents do not significantly change the Stokes shift. Both methods give comparable results and predict the shifts quite well for the molecules we investigated.
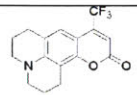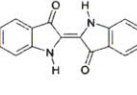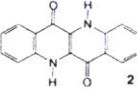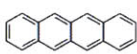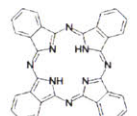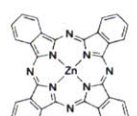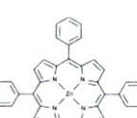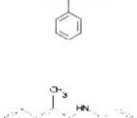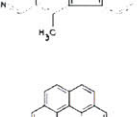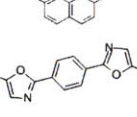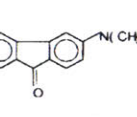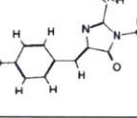
Dye	Structure	Environment	Experimental Stokes Shift (eV)	TDDFT Stokes Shift (eV)	ΔSCF Stokes Shift (eV)	Ref.
1		Gas Phase	0.44	0.51	0.42	[7]
2		Gas Phase	0.10	0.60	0.14	[8]
3		Gas Phase	0.19	0.16	0.21	[8]
4		Gas Phase	0.36	0.34	0.32	[9]
5		Cyclohexane	0.17	0.41	0.40	[10]
6		Gas Phase	0.00	0.08	0.12	[11]
7		Gas Phase	0.02	0.07	0.10	[11]
8		Benzene	0.34	0.20	0.32	[12]
9		Hexane	0.15	0.31	0.35	[13]
10		Gas Phase	0.23	0.12	0.36	[14]
11		Octane	0.43	0.40	0.55	[15]
12		Cyclohexane	0.57	0.69	0.72	[16]
13		Gas Phase	0.68	0.60	0.53	[17],[18]

Table 1. Test set of dyes: chemical structures, environment, experimental Stokes shifts, and theoretical Stokes shifts (calculated using ΔSCF with the B3LYP functional and the 6-31G* basis set).

We computed test statistics for this set of calculations (see Table 2) and the mean error and mean absolute errors appear favorable, since the intrinsic accuracy of DFT is around 0.3 eV. However, there is no indication of a systematic overestimation or underestimation by either ΔSCSF or TDDFT.

Method	Mean Error	Mean Absolute Error	Root Mean Standard Deviation
ΔSCF	0.07	0.10	0.12
TDDFT	0.07	0.13	0.18

Table 2. Statistics for the test set of ΔSCF calculations. Units are electron-volts.

Since some of the experimental numbers were measured in solvents, we have separated the gas phase (Table 3) and solution phase (Table 4) dyes and looked at the accuracy of ΔSCF and TDDFT in each case. All calculations were done excluding solvent effects. These tables also show the individual absorptions and emissions of each molecule.

Dye Number	Dye	Medium	Experimental			ΔSCF			TDDFT		
			Absorption (eV)	Emission (eV)	Stokes Shift (eV)	Absorption (eV)	Emission (eV)	Stokes Shift (eV)	Absorption (eV)	Emission (eV)	Stokes Shift (eV)
10	Coronene	Gas Phase	3.05	2.82	0.23	3.68	3.32	0.36	3.46	3.34	0.12
1	Coumarin 153	Gas Phase	3.37	2.93	0.44	3.16	2.74	0.42	3.36	2.85	0.51
3	DBNPD	Gas Phase	3.01	2.82	0.19	2.93	2.72	0.21	3.11	2.95	0.16
6	H2Pc	Gas Phase	1.80	1.80	0.00	1.93	1.81	0.12	2.09	2.01	0.08
2	Indigo	Gas Phase	2.30	2.20	0.10	1.99	1.84	0.14	2.31	1.71	0.60
13	pHBDI	Gas Phase	3.12	2.44	0.68	3.10	2.58	0.53	3.55	2.94	0.60
4	Tetracene	Gas Phase	2.92	2.56	0.36	2.45	2.13	0.32	2.49	2.16	0.34
7	ZnPc	Gas Phase	1.88	1.86	0.02	1.91	1.81	0.10	2.09	2.03	0.07

Table 3. Experimental and theoretical Stokes shifts for dyes in the gas phase. Dye numbers refer to Table 1. All ΔSCF and TDDFT calculations were performed in the gas phase using the B3LYP functional and the 6-31G* basis set.

Dye Number	Dye	Medium	Experimental			ΔSCF			TDDFT		
			Absorption (eV)	Emission (eV)	Stokes Shift (eV)	Absorption (eV)	Emission (eV)	Stokes Shift (eV)	Absorption (eV)	Emission (eV)	Stokes Shift (eV)
12	3DMAF	Cyclohexane	3.10	2.53	0.57	3.02	2.30	0.72	3.02	2.33	0.69
9	Ellipticine	Hexane	3.25	3.10	0.15	3.39	3.04	0.35	3.39	3.08	0.31
11	POPOP	Octane	3.46	3.03	0.43	2.99	2.44	0.55	3.19	2.79	0.40
5	Rubrene	Cyclohexane	2.39	2.22	0.17	2.16	1.76	0.40	2.18	1.77	0.41
8	ZnTPP	Benzene	2.26	1.92	0.34	2.46	2.15	0.32	2.30	2.11	0.20

Table 4. Comparison of gas phase ΔSCF and TDDFT calculations to experimental measurements done in solution. Dye numbers refer to Table 1. All ΔSCF and TDDFT calculations were performed using the B3LYP functional and the 6-31G* basis set.

Performing error analysis separately on the gas phase and the solution dyes indicates that ignoring the solvent effects in our calculations may be a minor source of error (Tables 5 and 6). Overall, these calculations confirmed our assumption that nonpolar solvent effects for these dyes would be insignificant.

Dyes in Gas Phase		
	ΔSCF	TDDFT
Mean Error	0.02	0.08
Mean Absolute Error	0.08	0.12
RMSD	0.09	0.19

Table 5. Error analysis for ΔSCF and TDDFT calculations for gas phase dyes. All units are electron-volts.

Dyes in Solution		
	ΔSCF	TDDFT
Mean Error	0.14	0.06
Mean Absolute Error	0.14	0.14
RMSD	0.16	0.17

Table 6. Error analysis for gas phase ΔSCF and TDDFT calculations for dyes with experimental Stokes shifts measured in solution. All units are electron-volts.

2.4   Conclusions

The calculation of electronic excited states is very beneficial for studying molecules that could be used in renewable energy sources, particularly for solar energy. Since these molecules store and release energy via their absorption and emission processes, it is important that we have a good understanding of how these molecules absorb and emit light and in what wavelength regime. Looking at Stokes shifts allows us to compare the relative absorption and emission spectra for each molecule and allows us to predict the compounds that might work better for any given application. For the calculation of Stokes shifts, ΔSCF has proven to be comparable to TDDFT and reproduces experimental results accurately. In addition, it could reduce the expense of doing excited state calculations, which would allow us to tackle larger chemical systems.

Chapter 3

A New Approach to Finding Reaction Pathways

3.1 Introduction

Transition states play a major role in chemistry as they are necessary for the calculation of reaction rates and lend significant insight into the way that reactions occur. Due to their importance, the identification of minimum energy paths (MEPs) for reactions is an active area of research and many optimization algorithms currently exist.

Reaction pathway mapping can be broken down into two main categories: pathway optimization and transition state optimization. For transition state optimization methods, the transition state is first optimized and then paths to the reactant and product states are subsequently determined. For pathway optimization however, it is assumed that there is no prior knowledge of the transition state. These pathway optimization methods can also be categorized into single minima methods and two minima methods, depending on whether both initial and final states are known, or if only one minimum on the potential energy surface (PES) is used. A common single minima method is the path of slowest ascent [19]. Two typical categories of two minima methods are the reaction coordinate (or 'drag') methods and chain-of-states methods. In reaction coordinate methods, a progress variable is defined (frequently through linear interpolation) between the product and reactant configurations. At each step, the remaining degrees of freedom are minimized over [20]. Figure 4 illustrates the "family tree" of reaction path finding.

```
┌─────────────────────────────────────────────────────────────────┐
│                    Reaction pathway mapping                       │
│                         ╱         ╲                               │
│          Pathway optimization        Transition state optimization│
│              ╱        ╲                                            │
│     Single minima      Two minima                                 │
│         ╱                ╱    ╲                                    │
│  Path of slowest ascent  Chain-of-states   Reaction coordinate    │
│                                               ('drag')            │
└─────────────────────────────────────────────────────────────────┘
```
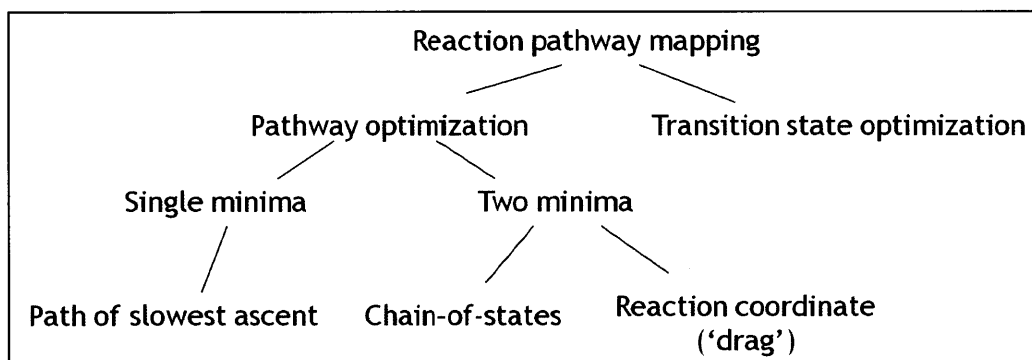
Figure 4. Tree diagram of major methods for reaction pathway mapping.

The chain-of-states methods are perhaps the most efficient and widely used today. In chain-of-states methods, a chain of images is generated between the two end points. The intermediate images are then optimized simultaneously to yield a path closer to the MEP. Note that these methods are not guaranteed to converge to the exact MEP. One major benefit of this method is that the distribution of states can be controlled allowing the density of images to be made higher in the critical region, i.e. more replicas can be created closer to the saddle point.

The nudged elastic band method (NEB) is an example of a chain-of-states method in which the chain of images is connected by springs. NEB is characterized by "nudging" which involves projecting out the perpendicular component of the spring force and the parallel component of the true force. This means that only the component of the spring force that lies along the tangent to the path is included. NEB has been shown to be an effective method for finding transition states with the caveat that it requires a reasonable initial guess for the path. [20]

Another method which has been widely used for constructing transition state paths is the string method which works by evolving "strings" or smooth parameterized curves. [21] Instead of using a spring force to connect the images, the states are repositioned to be equally spaced along the path after each optimization cycle. [22] Like NEB, this works well for smooth potential energy surfaces, but struggles to accurately capture reaction pathways along more rough, complicated landscapes. [21] Again, it is highly likely that starting with a better guess path would improve the convergence of the string method.

To summarize, the majority of existing path-finding methods are costly and more importantly, hard to converge. We could avoid performing many of the expensive iterations involved in these methods if we had a way to generate a good initial guess for the path.

3.2   Generating a New Initial Guess

Since no systematic method for making this initial guess has previously been developed, we have created a precursory path-finding method utilizing the information we have about the properties of the true MEP. We begin by assuming that we have two optimized geometries, A and B, which serve as the initial and final configurations for our reaction, and for which we can calculate energies, gradients, and hessians. We can make these assumptions because the gradient of the energy should be zero at a local minimum, and hessians are widely available for electronic structure methods.

We also know that the path consists of initial and final endpoints, $\vec{q}_i$ and $\vec{q}_f$, and that it can be parameterized by a variable s that ranges from 0 to 1. Furthermore, we know that along the path, the derivative, $\frac{d\vec{q}}{ds}$, must be parallel to the gradient of the potential energy surface. At the endpoints, $\frac{d\vec{q}}{ds}$ must be parallel to the eigenvectors of the Hessian, x_i and x_f. Thus we have four constraints for our path, which we can express mathematically as follows.

- Condition 1: $\vec{q}(s = 0) = \vec{q}_i$

- Condition 2: $\vec{q}(s = 1) = \vec{q}_f$

- Condition 3: $\frac{d\vec{q}}{ds}(s = 0) = a\vec{x}_i$

- Condition 4: $\frac{d\vec{q}}{ds}(s = 1) = b\vec{x}_f$

We can now write down a functional form for our guess path by choosing a linear combination of trigonometric functions that satisfies these four conditions.

$$\vec{q}(s) = \frac{1}{2}(\cos(\pi s) + 1)\vec{q}_i + \frac{1}{2}(1 - \cos(\pi s))\vec{q}_f + \frac{a}{2\pi}\left(\sin(\pi s) + \frac{1}{2}\sin(2\pi s)\right)\vec{x}_i + \frac{b}{2\pi}(\sin(\pi s) - \frac{1}{2}\sin(2\pi s))\vec{x}_f$$

(Eqn. 1)
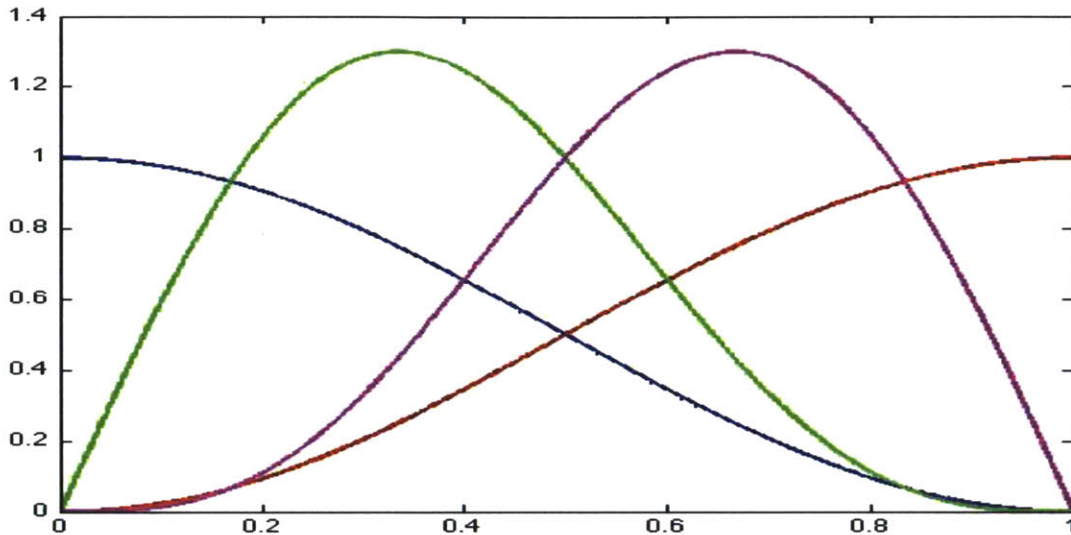
Figure 5. The trigonometric functions which serve as the bases for our guess path. The blue curve represents the first cosine term in equation 1, the red curve represents the second cosine term, and the green and purple curves represent the first and second sine terms, respectively.

Using trigonometric functions not only allows us to treat the initial and final points symmetrically, but also provides a one-to-one correspondence between the terms in our path equation and the conditions that they satisfy. Each basis function is a smooth curve (Figure 5), and thus a linear combination of these trigonometric terms provides a smooth path between the initial and final points.

3.3   Test Systems

3.3.1   Müller-Brown Potential Energy Surface

We began testing our guess path by applying it to the simple and well known Müller-Brown potential energy surface [23] and hand selecting the appropriate eigenvectors while varying the parameters, *a* and *b* (see Figure 6). The potential for the Müller-Brown surface can be written down analytically as seen in Equation 2:

$$MB(x,y) = \sum_{i=0}^{3} A_i e^{c_j(x-x_j^0)^2 + d_j(x-x_j^0)(y-y_j^0) + f_j(y-y_j^0)^2}$$ **(Eqn. 2)**

where A = [-200, -100, -170, 15], c = [-1, -1, -6.5, 0.7], d = [0, 0, 11, 0.6], f = [-10, -10, -6.5, 0.7], x^0 = [1, 0, -0.6, -1], y^0 = [0, 0.5, 1.5, 1].
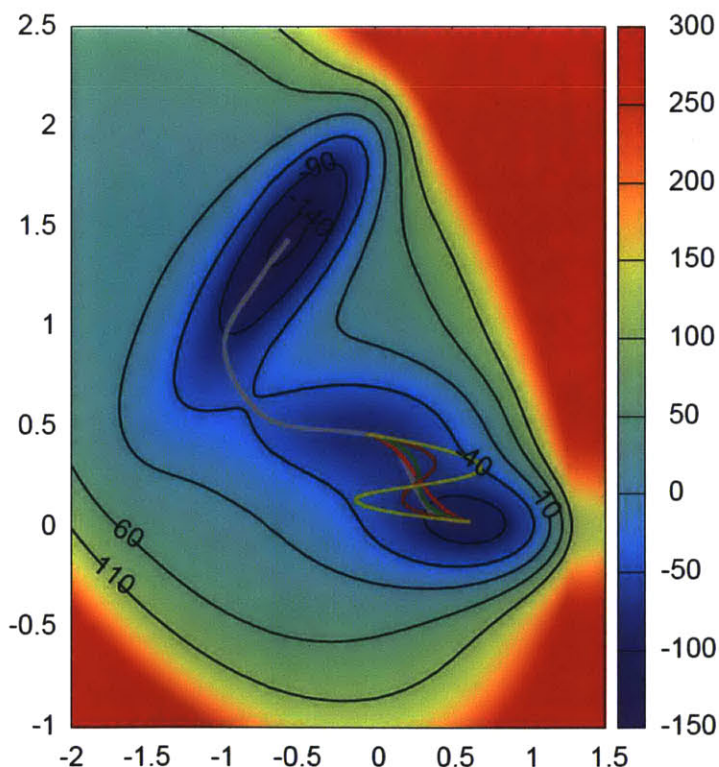
Figure 6. The linear combination of trigonometric functions is used as a guess path for the Müller-Brown surface. The gray curve represents the internal reaction coordinate for this potential and every other curve represents a different pair of *a* and *b* parameter choices.

It is apparent from Figure 6 that by changing the *a* and *b* parameters we can tune the curvature of the path and create a family of curves that vary in their proximity to the true path. In addition, it appears that by choosing the *a* and *b* parameters wisely, we can come up with a good estimate for the path.

3.3.2 Wolfe-Quapp Potential Energy Surface

As an additional test case, we used another two dimensional analytical potential surface known as the Wolf-Quapp potential [24]. This potential can also be expressed mathematically as follows:

$$WQ(x, y) = x^4 + y^4 - 2x^2 - 4y^2 + xy + 0.3x + 0.1y \quad \textbf{(Eqn.3)}$$

This potential provides a slightly more interesting case in that it has three distinct minima, with a saddle point in the center. In Figure 7, we demonstrate another family of curves generated using two minima from the Wolfe-Quapp surface, our guess path formula, and a variety of *a* and *b* parameters.
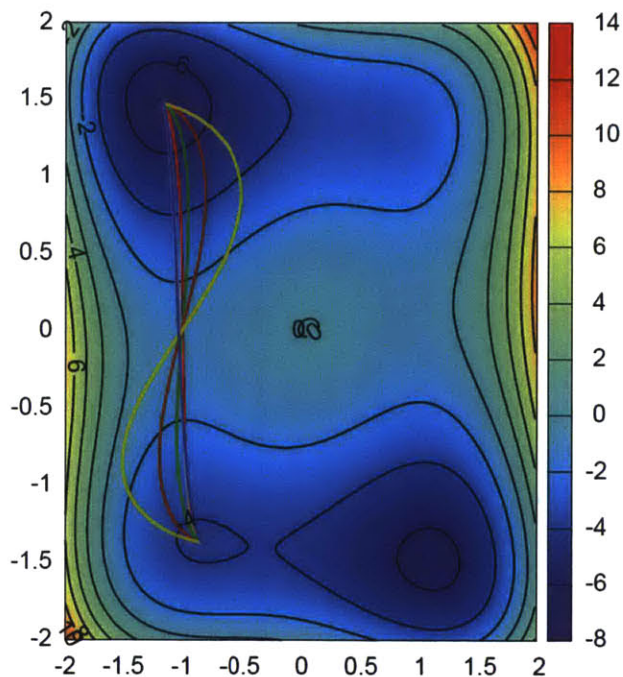
Figure 7. The trigonometric functional form is used to create a guess path for the Wolfe-Quapp surface. The gray curve represents the internal reaction coordinate for this potential while every other curve represents a different pair of *a* and *b* parameter choices .

Figure 7 again demonstrate that by appropriately choosing a and b we can generate guess paths that closely resemble the true path connecting the minima on the potential energy surface. We now want to come up with a systematic method for optimizing a and b. While there may be many approaches to solving this problem, we choose to minimize the maximum potential (i.e., we scan over a grid of a and b values and choose the ones that generate the lowest barrier height). This simple solution works well for us because we are using the exact potential along the path. At this point we are just trying to show that we can generate an accurate path for simple test cases, but this optimization method could also be used in more difficult examples where we can approximate the potential along the path using an electronic structure or similar method.

Figure 8 illustrates the results of this optimization method. In the top two plots we are able to reproduce almost exactly the true path connecting the minima. Starting search for a and b at the same values when connecting the last two minima results in a guess path that goes through the highest barrier possible, however (bottom left of Figure 8). This issue can be resolved by choosing a better starting point for the a and b parameter scan as shown in the bottom right plot of Figure 8.
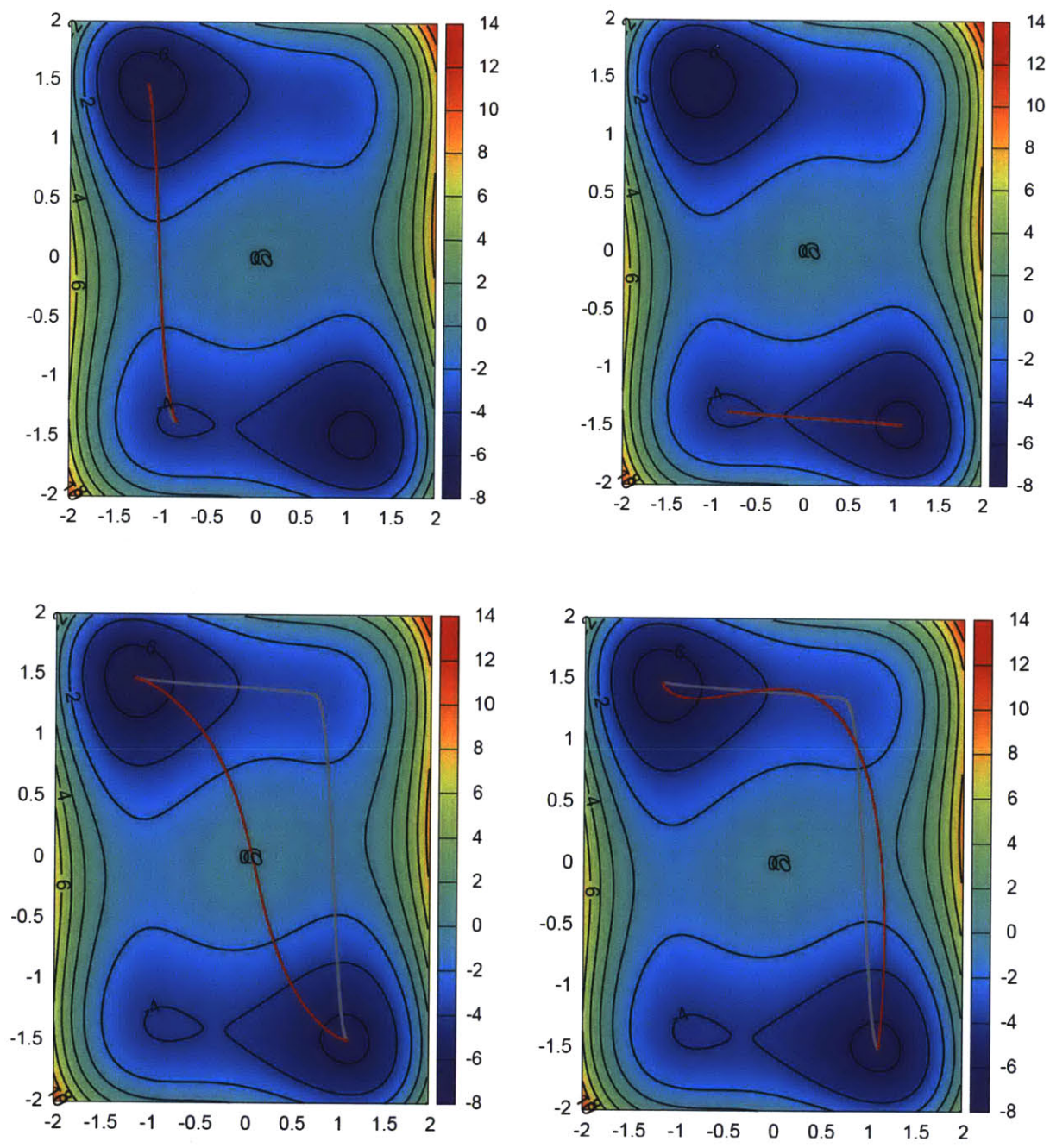
Figure 8. The *a* and *b* parameters in the functional form of our guess path are optimized by minimizing the barrier height along the path. For most cases this results in a nearly perfect reproduction of the true path. In the bottom left case however, a closer estimate of the correct *a* and *b* parameters was necessary before optimizing in order to avoid the saddle point (bottom right).

3.3.3   Quapp-Hirsch-Heidrich Potential Energy Surface

The Quapp-Hirsch-Heidrich potential energy surface is an effectively two dimensional surface which we tested as yet another confirmation of our function's ability to reproduce basic reaction paths. Equation 4 gives the functional form for the Quapp-Hirsch-Heidrich potential [25].

$$QHH(x,y,z) = 2y + y^2 + (y + 0.4x^2 + z^2)x^2 + 0.01z^2 \quad \textbf{(Eqn. 5)}$$
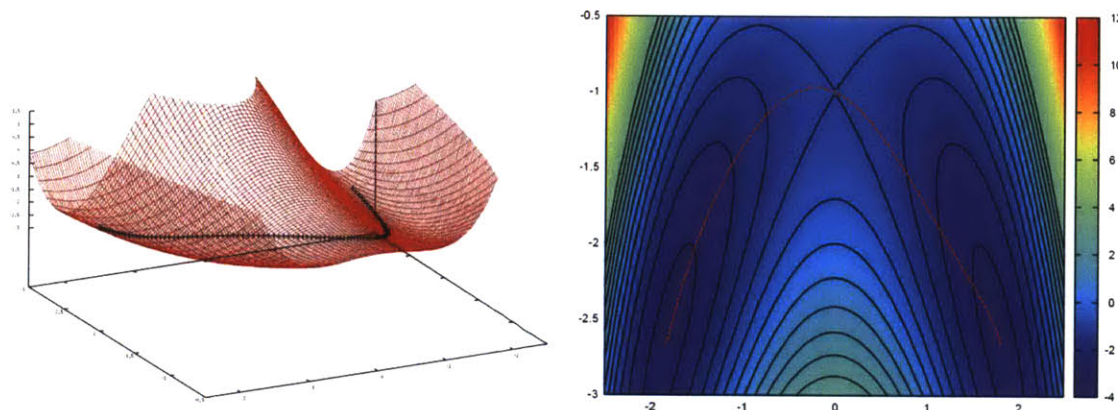
Figure 9. Plot of the minimum energy path found using our trigonometric form connecting the minima on the Quapp-Hirsch-Heidrich surface. On the left is a surface plot with our guess path indicated in black, and on the right is a contour plot with our guess path in red. Both images are plotted along the z=1 isosurface.

Again we see that our function performs admirably, and the optimization of the a and b parameters results in a path that passes close to the true transition state barrier.

3.3.4   Cosine Potential

To move to a slightly more complicated test case, let us now consider a three particle system where the interaction between any two particles is given by a simple cosine potential:

$$V = \frac{\cos(r_{ij})}{r_{ij}^2} \quad \textbf{(Eqn. 6)}$$

where r_{ij} is the interatomic distance between particles i and j.
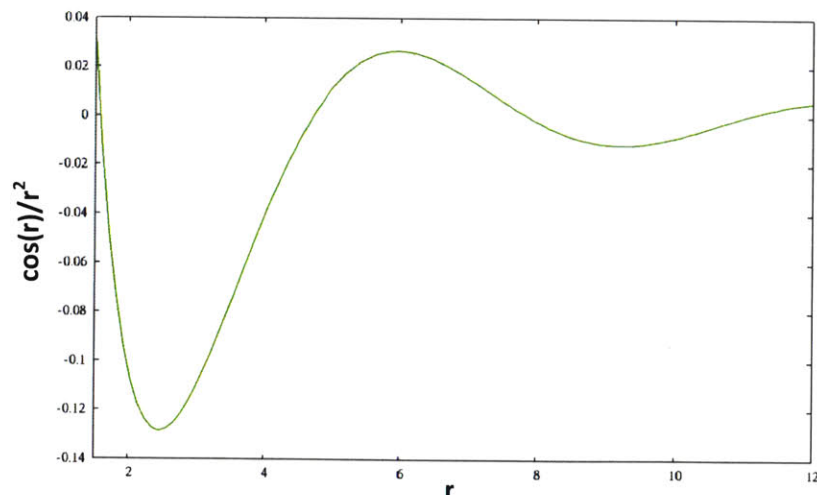
Figure 10. The cos(r)/r² is plotted on the y axis for a range of r values on the x axis.

This potential has several minium, but we will look at the case where the three particles begin in the first well with a short interatomic distance, and stretch to the next well where they all have slightly longer interatomic distances. We can roughly think of this as atoms initially connected by "double" bonds stretching into "single" bonds. The intial and final states are indicated in Figure 11.
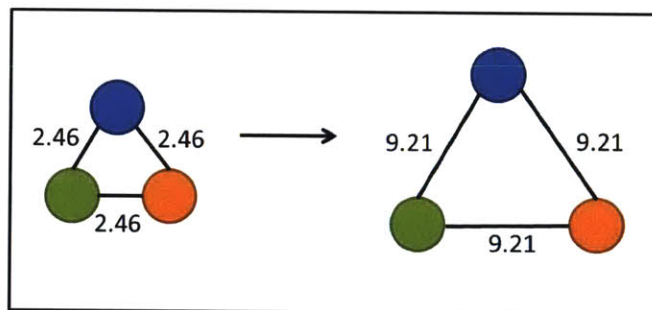
Figure 11. A three particle system stretching from short bond distances to longer bond distances. Both the initial and final geometries are local minima for our cosine potential.

When we convert the formula for our potential into Cartesian coordinates and apply our method, we find that we generate a guess path with two barriers (Figure 12). This is promising because the true reaction path for this potential also has two barriers. Our guess path slightly overestimates the first barrier (for which the correct value is indicated by the blue line in Figure 12) and the intermediate (indicated by the green line). We reproduce the second barrier correctly (shown by the purple line in Figure 12).

26
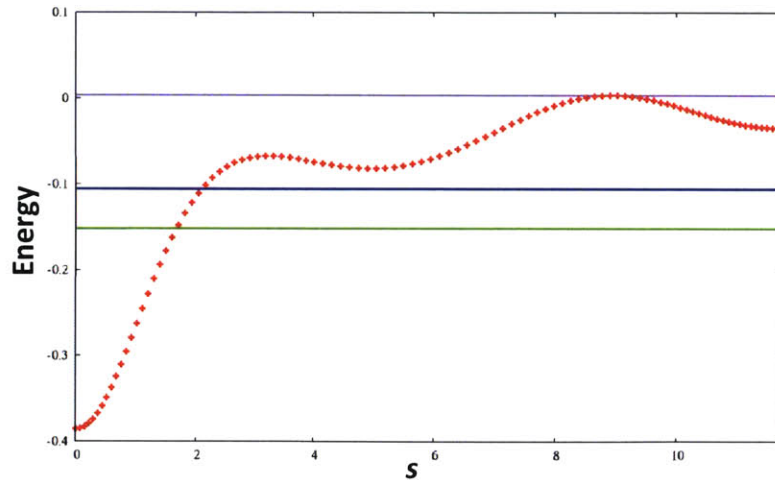
Figure 12. The guess path generated for our cosine potential when the optimization is performed in Cartesian coordinates. Several features of the true path are indicated- the blue line indicates the energy at the first barrier, the green line indicates the energy at the intermediate, and the purple line represents the energy at the second barrier.

We can also observe the motion of the particles for this path (Figure 13). Ideally, one particle (red) should into its new position first, while a second particle (green) moves just enough to obey the triangle inequality. After the first particle has reached its final position, the second particle should finish its movement, thus creating the second barrier. The third particle (blue) should remain fixed for the entire process. This mechanism results in a minimization of energy at every point along the path. The guess path pictured in Figure 13 exhibits behavior very close to what we expect, thus affirming that our method works well for simple particle motions.
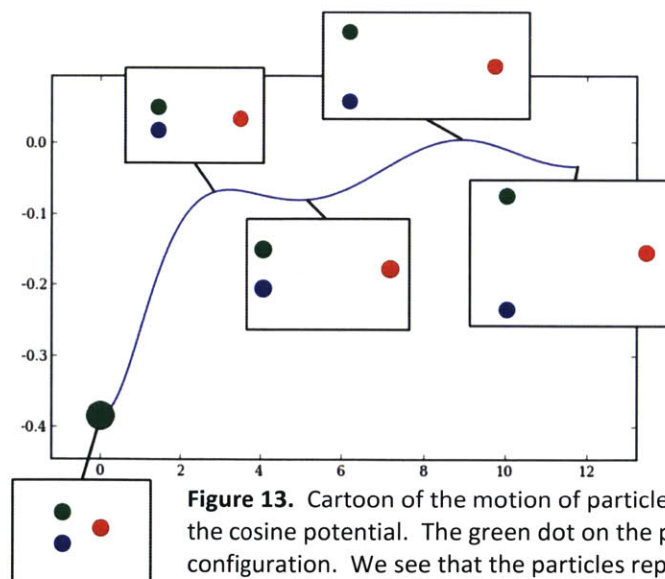
Figure 13. Cartoon of the motion of particles along our guess path for the cosine potential. The green dot on the path indicates the starting configuration. We see that the particles reproduce the expected movements almost exactly.

3.3.5   Seven Atom Lennard-Jones Cluster

Moving towards even more complicated systems, we apply this method to the rearrangement of a seven atom Lennard-Jones cluster in two dimensions [26]. This will give us some idea of how our method will work for a more realistic chemical system. In the cluster, the interaction between any two particles is governed by a typical Lennard-Jones potential (Equation 7).

$$LJ = 4\varepsilon \left[\left(\frac{\sigma}{r} \right)^{12} - \left(\frac{\sigma}{r} \right)^{6} \right] \quad \textbf{(Eqn. 7)}$$

In this equation, r is the interatomic distance between any two particles. For our system, we chose $\varepsilon=1$ and $\sigma=2^{5/6}$. We have chosen a reaction where we take the central particle in the cluster and exchange it with one of the particles in the outer ring. Converting our potential into Cartesian coordinates, we can use our method to generate a guess path. The initial and final configurations for our cluster and our guess path are pictured in Figure 14a.

In calculating reaction paths for this Lennard-Jones cluster, we encounter an interesting problem. Depending on the order in which the particles are numbered, we generate different "best" paths for the system. Since there are 7! possible orderings, this creates a lot of paths to search through to find the path with the lowest barrier. Figure 14 illustrates two of the paths that we can create by changing the indexing of the particles. The paths are qualitatively and quantitavely different as the second path (Figure 14b) has three barriers as opposed to one, and the barrier heights are about two Lennard-Jones energy units higher than the path generated in Figure 14a. It is important, therefore, to use one's intuition about the motion of the particles along the path to index the particles in such a way as to minimize the required movement of the particles thereby minimizing the energy needed to reach the final configuration.
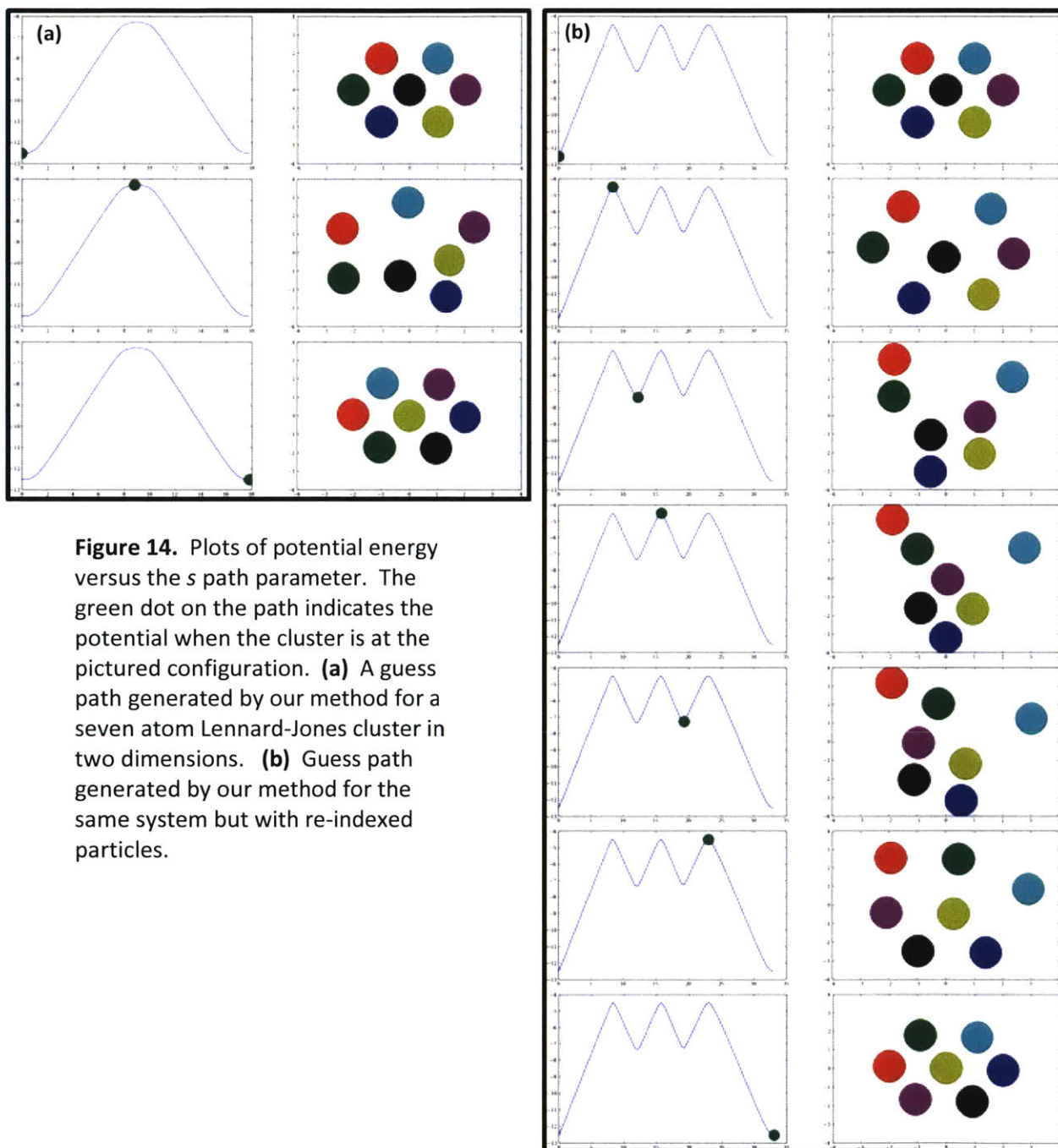
Figure 14. Plots of potential energy versus the *s* path parameter. The green dot on the path indicates the potential when the cluster is at the pictured configuration. **(a)** A guess path generated by our method for a seven atom Lennard-Jones cluster in two dimensions. **(b)** Guess path generated by our method for the same system but with re-indexed particles.

After generating an initial guess path, we can use the estimated barrier to refine the path. For example, if we find a path with one barrier, we can break that path up into two pieces, creating a path from the initial configuration to the intermediate, and another from the intermediate to the final configuration. We can then apply our path-finding method to each piece and concatenate the new guess paths to create a better path for the overall reaction.

Figure 15 illustrates an example of this process, where the path pictured on the left is the initial reaction proposed by our method and the path on the left is a refined path created by recalculating paths between the initial geometry and the intermediate, and the intermediate and the final geometry. Applying this algorithm just once qualitatively changed the potential profile along the path as well as lowering the energy by about four Lennard-Jones units. This process could be repeated until another iteration no longer lowers the barrier height.

If indices are chosen wisely, and the intermediate found is used to refine the path, our method can very reasonable reaction pathways for the Lennard-Jones system which shows promise for real chemical systems.

Figure 15. The illustration on the left shows a guess path generated using only the initial and final configurations with a particular set of indices for our Lennard-Jones cluster. This path was then refined by using the intermediate and the new path is shown on the right. The potential profile has changed qualitatively and the energy was lowered by about 4 Lennard-Jones units.

3.4   Dependence on Choice of Coordinate System

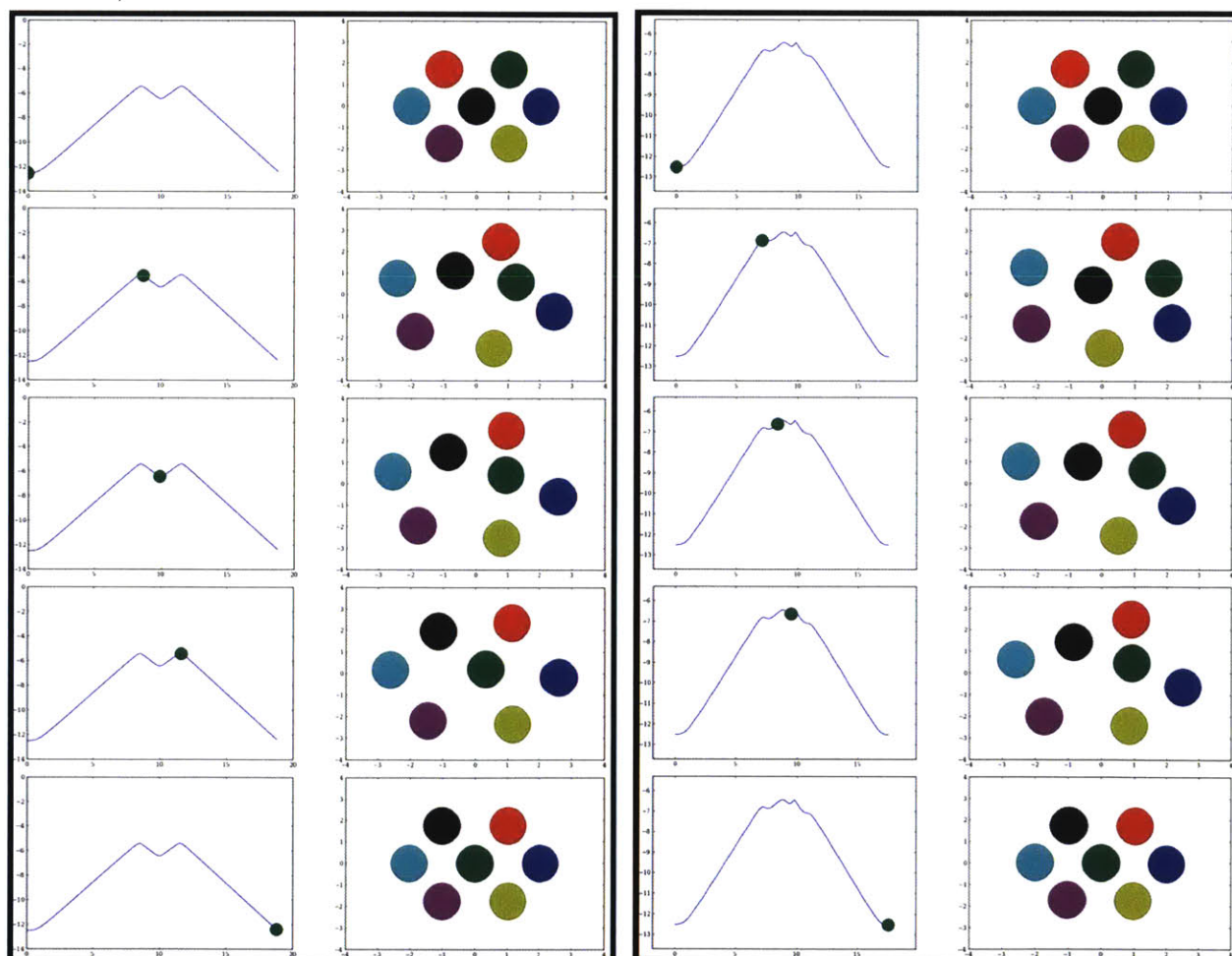Besides the choice of indices used for cluster-type systems, the paths that we are able to generate using our method can also change depending on which coordinate system we perform our optimization in. This makes intuitive sense, since most electronic structure methods choose not to use Cartesian coordinates, but a set of internal coordinates for better geometry optimizations. To see how large of a role the choice of coordinate system played in our method, we revisited the cosine potential and seven atom Lennard-Jones cluster with different choices of coordinates.

3.4.1   Cosine Potential

In Section 3.3.4 we approximated a reaction path for a three particle system whose interactions were governed by the cosine potential in Equation 6. There we performed the calculations using Cartesian coordinates.

Here, we use the same potential, but we recalculate the guess path using interatomic distances and internal coordinates. Figure 16 illustrates our simple choice for internal coordinates for this system of two interatomic distances and an angle.
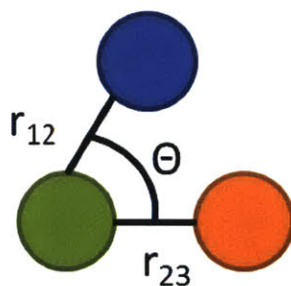
Figure 16. For our three particle system, we choose internal coordinates consisting of two interatomic distances, r_{12} and r_{23} and an angle, Θ.

The results of these optimizations can be seen in Figure 17. In the top plot we show our original calculation of the path using Cartesian coordinates. The middle plot is the optimization performed using interatomic distances, and the bottom plot is the path generated by using the interal coordinate scheme in Figure 16. In all three plots the blue, green, and purple lines

indicate the correct energy levels of the first barrier, intermediate, and the second barrier, respectively. The Cartesian coordinates are the only ones that reproduce a qualitatively correct path with two barriers. The internal coordinates are clearly the worst choice, since they result in a path with a strange and unrealistic cusp. All three paths do manage to get some of the energetics right, however. This figure definitely confirms that the choice of coordinate system makes a significant difference in the predicted path.
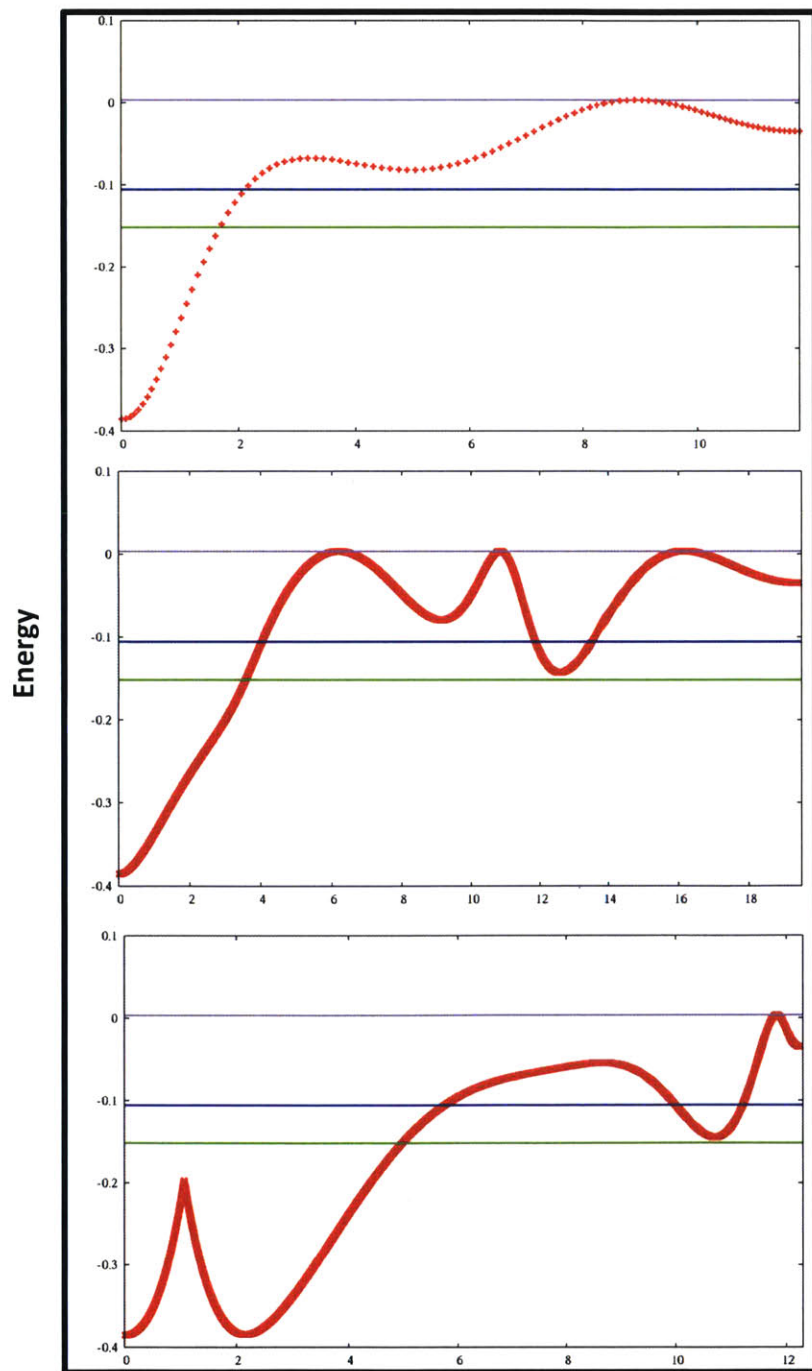
Figure 17. Three predicted paths for the cosine potential in Section 3.3.4. The top plot is the best path determined using Cartesian coordinates, and the middle and bottom plots are the optimized paths generated using interatomic distances and internal coordinates, respectively. The Cartesian coordinates produce the most qualitatively and quantitatively accurate path.

3.4.2   Seven Atom Lennard-Jones Cluster

Since the Lennard-Jones potential lends itself to calculations in interatomic distances, we chose to compare the path predicted by our method in interatomic distances to the path using Cartesian coordinates in Section 3.3.5. The path optimized using interatomic distance is shown below (Figure 18).
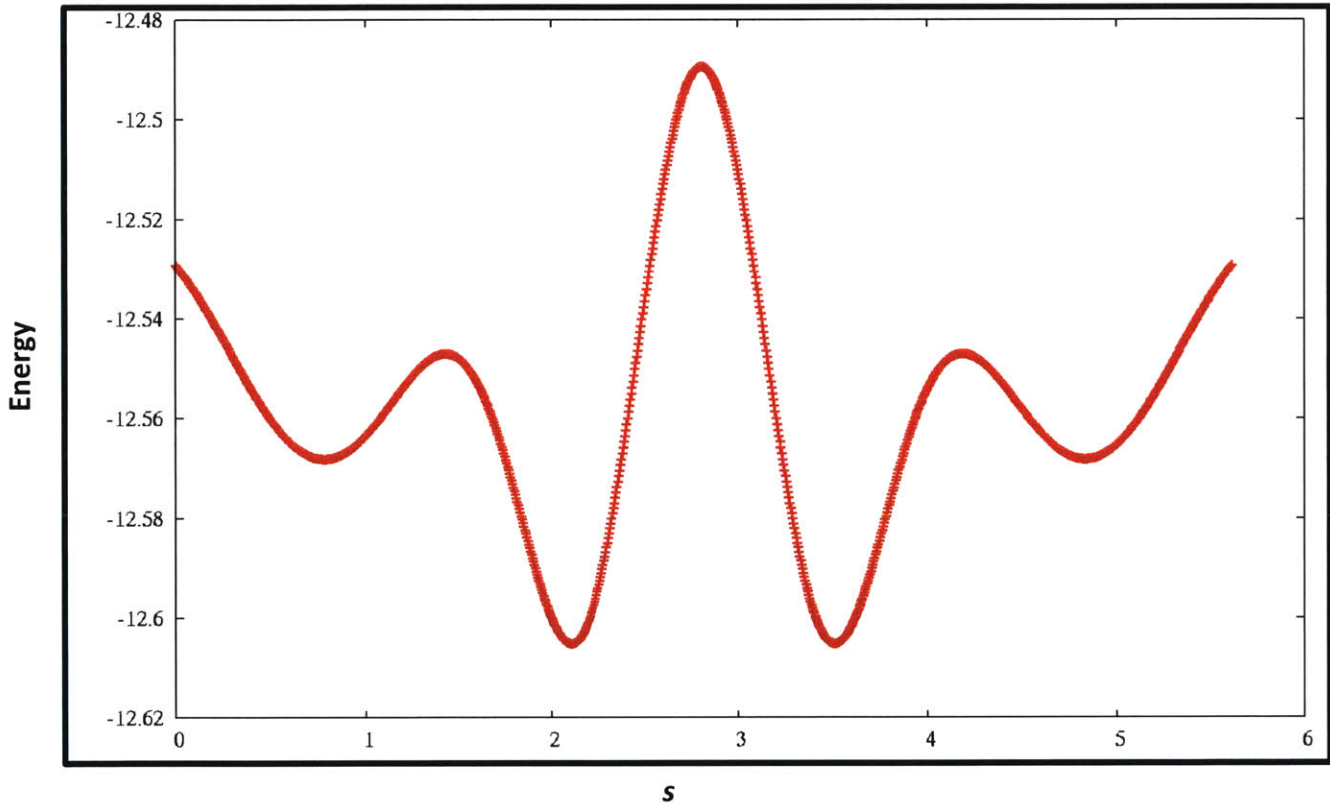
Figure 18. A plot of potential energy (in Lennard-Jones units) versus the *s* path parameter. This guess path was generated by performing the optimization using interatomic distances.

In the case of the seven atom Lennard-Jones cluster, we run into significant problems. As illustrated in Figure 18, the potential predicted by our method dips way below the energy at the endpoints (i.e. the energy along the path is lower than the energy at the minima)! This is due to the fact that interatomic distances are a redundant set of coordinates for this system. In other words, the configuration is overdetermined. This results in the cluster satisfying the triangle equality in higher dimensions than we physically have access too. Thus, the Cartesian coordinates are again the better choice for this system.

3.5   Conclusions

Since transition states play such a vital role in chemistry, it is important to have an accurate way to predict reaction pathways and barrier heights. We have developed a method of constructing a guess path using a simple trigonometric form for the path function. We have demonstrated its ability to accurately predict the path for analytical potential energy surfaces ranging from simple two dimensional test cases to more complicated cluster rearrangements. It is clear that some intuition is necessary for determining the most accurate path, however. We must be able to make a wise choice of eigenvectors to use, and have a reasonable initial guess to start the optimization of the a and b parameters. As demonstrated by the cosine and Lennard-Jones potentials, the choice of coordinate system makes a significant difference in the qualitative and quantitative properties of the path. In the cases that we examined, Cartesian coordinates appeared to be the best choice, but this could change depending on the system. A well-chosen set of internal coordinates could be the best choice for many systems. Intermediates can also be used to further refine the path. Overall, though, this method is an excellent scheme for generating an approximate reaction path given initial and final geometries with their energies, gradients, and hessians. Our guess path could be used as a better starting point for other path-finding methods such as the nudged elastic band method, to help speed up convergence and reduce the number of more costly iterations needed.

Chapter 4

Conclusions

Solar energy has been a popular research topic lately, particularly in materials laboratories. Creating materials that can efficiently store energy from the sun would be a huge step in utilizing all of the sunlight that is reflected back into the atmosphere. Theoretical chemistry has a unique opportunity to contribute to this research. By utilizing our ability to predict trends and test properties of new materials before they are able to be synthesized in a lab, we can supply experimentalists with promising directions to explore. Both theory and experiment play a huge role in the development of materials, and by working together scientists from both backgrounds can make amazing progress.

We have shown that ΔSCF is a promising way to compute Stokes shifts. It would be very beneficial to use ΔSCF to study the behavior of molecules with large Stokes shifts, since these systems are often used in fluorescent solar concentrators. Since ΔSCF is less expensive and as accurate for large molecules as TDDFT, it would interesting to explore how it performs for other electronic properties of materials. ΔSCF could also be used to investigate vibronic transitions and Franck Condon factors which describe the overlap of vibrational wave functions.

We have found that we can use the information that we know about the endpoints in a reaction to generate a good estimate for the path between them using a simple combination of trigonometric functions. It is important to choose a coordinate system and particle indices wisely, where appropriate, but we have seen that our guess path reproduces the exact path very accurately for simple systems. Future work in this area would include applying our path finding method to real systems and other systems typically used as path finding benchmarks to see how well the model will work for practical applications [27]. The method could then be

implemented as a precursor to NEB or another more sophisticated path finding method to see if it improves the convergence and cost of the transition state search.

After pursuing these projects a bit further individually, the ΔSCF approach could be combined with the path finding method to explore excited state potential energy surfaces. Complications arise when treating reactions that occur in the excited state due to conical intersections [28]. Conical intersections are simply the intersections of two potential energy surfaces and often play a role when a molecule moves between an excited state and the ground state. When electrons are excited, in photoexcitation, for example, the electrons must eventually return to the electronic ground state. This contradicts the assumption of the Born-Oppenheimer approximation which says that the atoms move on a potential energy surface governed only by their atomic coordinates and Coulombic repulsion. The return to the ground state usually occurs at geometries where at least two electronic states have the same energy, and this constitutes a conical intersection [29]. Since conical intersections could play a role in solar thermal fuels, investigating them with ΔSCF to see how this method performs at these short-lived, energetically unstable geometries would be very useful After looking at ways to compute energies at conical intersections, both ΔSCF and our path finding method could be incorporated into an excited state transition state search method.

ΔSCF has the potential to be applied to some widely known photoswitching molecules. The electrons in these molecules are excited via exposure to light, and eventually 'cool' back down to the ground state. By looking at the way they behave in the excited state and during their transitions between the ground and excited state we may be able to glean important information about the properties of these solar fuels. Specifically it would be interesting to study more azobenzene derivatives and compare how the molecules in solution behave relative to the azobenzene derivatives covalently bound to carbon nanotubes. Other photoswitching molecules such as fulgides, azulenes, and diarylethenes both with and without carbon nanotube binding could also be explored [30]. This could give us new insight into choosing materials for solar thermal fuels.

In addition, combining the ΔSCF method with an efficient path finding tool would allow us to look at the dynamics and mechanics of the reactions that take place in photoswitching systems such as azobenzene derivatives covalently bonded to carbon nanotubes. This, in turn, would help us tune the properties of these materials and allow us to develop a more efficient solar thermal fuel.

References

[1] A.M. Kolpak and J.C. Grossman. Azobenzene functionalized carbon nanotubes as high-energy density solar thermal fuels. *Nano Letters*, DOI:10.1021/nl201357n, 2011.

[2] W.G.J.H.M. van Sark, et al. Luminescent solar concentrators – a review of recent results. *Optics Express*, 16:21773-21792, 2008.

[3] F. Vollmer, W. Rettig, and E. Birckner. Photochemical mechanisms producing large fluorescence Stokes shifts. *Journal of Fluorescence*, 4(1):65-69, 1994.

[4] E. Runge and E.K.U. Gross. Density-functional theory for time-dependent systems. *Physical Review Letters,* 52(12):997-1000, 1984.

[5] T. Ziegler, A. Rauk, and E.J. Baerends. On the calculation of multiplet energies by the hartree-fock-slater method. *Theoretica Chimica Acta,* 43(3):261-271, 1977.

[6] T. Kowalczyk, S.R.Yost, and T. Van Voorhis. Assessment of the ΔSCF density functional theory approach for electronic excitations in organic dyes. *The Journal of Chemical Physics,* 134(5):2011.

[7] N.P. Ernsting, M. Asimov, and F.P. Schafer. The electronic origin of the [pi][pi]* absorption of amino coumarins studied in a supersonically cooled free jet. *Chemical Physics Letters,* 91(3): 231-235, 1982.

[8] G. Hauke and G. Graness. Thermal isomerization of indigo. *Angewandte Chemie International Edition in English,* 34(1):67-68, 1995.

[9] R. Williams and GJ Goldsmith. Fluorescence of napththacene vapor. *The Journal of Chemical Physics,* 39:2008, 1963.

[10] F. Bayrakçeken. A new type of delayed fluorescence of rubrene in solution. *Journal of Luminescence,* 54(1):29-33, 1992.

[11] D. Eastwood, L. Edwards, M. Gouterman, and J. Steinfeld. Spectra of porphyrins: Part vii. Vapor absorption and emission of phthalocyanines. *Journal of Molecular Spectroscopy,* 20(4):381-390, 1966.

[12] H.-Z. Yu, J.S. Baskin, and A. H. Zewail. Ultrafast dynamic of porphyrins in the condensed phase: II. Zinc tetraphenylporphyrin. *Journal of Physical Chemistry A,* 106:9845-9854, 2002.

[13] S. Banerjee, A. Pabbathi, M.C. Sekhar, A. Samanta. Dual fluorescence of ellipticine: excited state proton transfer from solvent versus solvent mediated intramolecular proton transfer. *Journal of Physical Chemistry A,* 115(33): 9217-9225, 2011.

[14] T. Itoh. Multiple fluorescence and the electronic relaxation processes of coronene vapor: The fluorescence from the S1, S2, and S3 states. *Journal of Molecular Spectroscopy,* 252:115-120, 2008.

[15] A.O. Doroshenko, A.V. Kirichenko, V.G. Mitina, O.A. Ponomaryov. Spectral properties and dynamics of the excited state structural relaxation of the ortho analogues of POPOP – Effective abnormally large Stokes shift luminophores. *Journal of Photochemistry and Photobiology A: Chemistry,* 94:15-26, 1996.

[16] T. Yatsuhashi, Y. Nakajima, T. Shimada, and H. Inoue. Photophysical properties of intramolecular charge-transfer excited singlet state of aminofluorenone derivatives. *Journal of Physical Chemistry A,* 102:3018-3024, 1998.

[17] Y. Ma, M. Rohlfing, and C. Molteni. Modeling the excited states of biological chromophores within many-body Green's function theory. *Journal of Chemical Theory and Computation,* 6:257-265, 2010.

[18] T.M.H. Creemers, A.J. Lock, V. Subramaniam, T.M. Jovin, and S. Völker. Three photoconvertible forms of green fluorescent protein identified by spectral hole-burning. *Nature Structural Biology Letters,* 6(6):557-560, 1999.

[19] C.J. Cerjan and W.H. Miller. On finding transition states. *Journal of Chemical Physics,* 75(6):2800, 1981.

[20] H. Jónsson, G. Mills, and K.W. Jacobsen. Nudged elastic band method for finding minimum energy paths of transitions, in Classical and Quantum Dynamics in Condensed Phase Simulations, Ed. B.J. Berne, G. Ciccotti and D.F. Coker, 385 (World Scientific, 1998).

[21] W. E, W. Ren, and E. Vanden-Eijnden. String method for the study of rare events. *Physical Review B,* (66):2002.

[22] D. Sheppard, R. Terrell, and G. Henkelman. Optimization methods for finding minimum energy paths. *Journal of Chemical Physics,* 128:2008.

[23] K. Müller and L. Brown. Location of saddle points and minimum energy paths by a constrained simplex optimization procedure. *Theoretica Chimica Acta,* 53:75-93, 1979.

[24] W. Quapp. A growing string method for the reaction pathway defined by a Newton trajectory. *The Journal of Chemical Physics,* 122(17): 2005.

[25] W. Quapp, M. Hirsch, D. Heidrich. Bifurcation of reaction pathways: the set of valley ridge inflection points of a simple three-dimensional potential energy surface. *Theoretical Chemistry Accounts*:285-299, 1998.

[26] C. Dellago, P.G. Bolhuis, and D.Chandler. Efficient transition path sampling: Application to Lennard-Jones cluster rearrangements. *The Journal of Chemical Physics,* 108(22):9236-9245, 1998.

[27] S. Ghasemi and S. Goedecker. An enhanced splined saddle method. *The Journal of Chemical Physics*, 135:014108, 2011.

[28] I. Schapiro, F. Melaccio, E. Laricheva, and M. Olivucci. Using the computer to understand the chemistry of conical intersections. *Photochemical & Photobiological Sciences,* 10:867-886, 2011.

[29] T.J. Martinez. Physical chemistry: seaming is believing. *Nature,* 467:412-413, 2010.

[30] W. Browne and B. Feringa. Light switching of molecules on surfaces. *Annual Review of Physical Chemistry*, 60:407-428, 2009.